

SUSCEPTIBILITY OF COPPER TO GENERAL AND PITTING CORROSION IN SALINE GROUNDWATER

Timo Saario, Kari Mäkelä, Timo Laitinen, Martin Bojinov
VTT Manufacturing Technology

In STUK this study was supervised by **Juhani Hinttala**

The conclusions presented in the STUK report series are those of the authors and do not necessarily represent the official position of STUK.

ISBN 951-712-437-6
ISSN 0785-9325

Oy Edita Ab, Helsinki 2001

SAARIO Timo, MÄKELÄ Kari, LAITINEN Timo, BOJINOV Martin (VTT Manufacturing Technology).
Susceptibility of copper to general and pitting corrosion in saline groundwater. STUK-YTO-TR 176.
Helsinki 2001. 18 pp.

ISBN 951-712-437-6
ISSN 0785-9325

Keywords: copper, corrosion, surface films, nuclear waste

ABSTRACT

In Sweden and Finland the spent nuclear fuel is planned to be encapsulated in cast iron canisters that have an outer shield made of copper, which is responsible for the corrosion protection. In this work the susceptibility of Cu OFP to general and pitting corrosion was investigated in saline (1.45% Cl⁻) groundwater at T = 80 °C and p = 14 MPa using electrochemical techniques and weight loss measurements in autoclave conditions. The results were compared with earlier results gained in similar conditions but in highly saline (5.4% Cl⁻) groundwater. The conclusions presented here are strictly applicable only for the present case, where the groundwater was deoxygenated with nitrogen bubbling (ensuring dissolved oxygen level of lower than 5 mg/l) and where there was almost no mass transfer limitation for the corrosion products away from the surface. The main observations made are:

- The corrosion potential of Cu OFP in all test runs was in the range of $-0.10 \text{ V}_{\text{SHE}} < E_{\text{corr}} < 0.05 \text{ V}_{\text{SHE}}$, i.e. about 0.1 V higher than in the highly saline groundwater.
- At the corrosion potential active dissolution (corrosion) of Cu OFP takes place, as was the case in highly saline groundwater. However, the corrosion rate based on weight loss measurements of corrosion coupons was 0.014 mm/y, about 30% lower than in the highly saline groundwater.

SAARIO Timo, MÄKELÄ Kari, LAITINEN Timo, BOJINOV Martin (VTT Kemiantekniikka).
Kuparin alttiutta yleiseen ja paikalliseen korroosioon simuloitussa suolaisessa pohjavedessä.
STUK-YTO-TR 176. Helsinki 2001. 18 s.

ISBN 951-712-437-6
ISSN 0785-9325

Avainsanat: kupari, korroosio, pintafilmit, ydinjäte

TIIVISTELMÄ

Käytetty ydinpolttoaine on suunniteltu varastoitavaksi valurautasäiliöihin, joiden ulkopinnalle tulee kuparivaippa. Kuparivaippa toimii säiliön korroosiosuojana. Tässä työssä selvitettiin fosfori-mikroseostetun kuparin alttiutta yleiseen ja paikalliseen korroosioon suolaisessa (1.45% Cl⁻) pohjavedessä. Kokeellinen tutkimustyö tehtiin autoklaavissa lämpötilassa T = 80 °C ja paineessa p = 14 MPa käyttäen voltammetriaa, sähkökemiallista impedanssitekniikkaa, kontaktivastusmittaustekniikkaa sekä painohäviömittauksia. Mittaustuloksia verrattiin aikaisempiin, erittäin suolaisessa pohjavedessä (5.38 % Cl⁻) mitattuihin tuloksiin. Kokeelliset tulokset mitattiin olosuhteissa, joissa liuenneen hapen määrä oli alle 5 mg/l ja joissa korroosiotuotteiden massavirta pois päin näytteen pinnasta oli suhteellisen vapaa. Päätulokset ovat seuraavat:

- Fosfori-mikroseostetun kuparin korroosipotentiaali oli välillä $-0.10 \text{ V}_{\text{SHE}} < E_{\text{corr}} < 0.05 \text{ V}_{\text{SHE}}$, eli noin 0.1 V korkeampi kuin erittäin suolaisessa pohjavedessä.
- Fosfori-mikroseostettu kupari liukenee vapaassa korroosipotentiaalissa suolaiseen pohjaveteen. Korroosionopeus, perustuen kolmen korroosiokupongin painohäviömittauksien keskiarvoon oli 0.014 mm/vuosi, mikä on noin 30% pienempi nopeus kuin mitä aikaisemmissa mittauksissa on vastaavalla tavalla todettu erittäin suolaisessa pohjavedessä.

ACKNOWLEDGEMENTS

This work has been performed as part of the research program funded by the Swedish Nuclear Power Inspectorate (SKI) and Finnish Radiation and Nuclear Safety Authority (STUK) and aimed at verification of the safety of nuclear fuel waste disposal concept. The reports from this research program published earlier are

- 1 STUK-YTO-TR 105 (1996), "Environmentally assisted cracking behaviour of copper in simulated ground water",
- 2 STUK-YTO-TR 106 (1996), "Electrical properties of oxide films formed on copper in 0.1 M borax solution",
- 3 SKI Report 96:80 (1996), "The effect of nitrite ion on the electric properties of oxide films on copper",
- 4 STUK-YTO-TR 134 (1997), "The effect of chlorides on the electric properties of oxide films on copper",
- 5 SKI Report 99:27 (1999), "Surface films and corrosion of copper",
- 6 STUK-YTO-TR 157 (1999), "Electric and electrochemical properties of surface films formed on copper in the presence of bicarbonate ions", and
- 7 SKI Report 01:2 (2001), "Susceptibility of copper to general and pitting corrosion in highly saline groundwater".

The project reported here has been funded by STUK. Co-operation with senior inspector Juhani Hinttala, STUK, is gratefully acknowledged.

CONTENTS

ABSTRACT	3
TIIVISTELMÄ	4
ACKNOWLEDGEMENTS	5
CONTENTS	6
1 INTRODUCTION	7
2 EXPERIMENTAL	8
3 RESULTS AND DISCUSSION	9
3.1 Corrosion coupon tests	9
3.2 Voltammetry and polarisation resistance	10
3.3 Electric resistance of surface	12
3.4 Impedance response of copper	13
4 CONCLUSIONS	17
REFERENCES	18

1 INTRODUCTION

In Sweden and Finland the spent nuclear fuel is planned to be encapsulated in cast iron canisters that have an outer shield made of copper. The copper shield is responsible for the corrosion protection of the canister construction.

The pressure in the final disposal vault is built up by two components. The first part consists of the hydrostatic pressure of water. This part depends on the depth at which the vault is built. If the vault is at the depth of 700 m, the hydrostatic pressure increases up to 7 MPa. The bentonite clay surrounding the copper canister will swell when it is wetted. This causes an additional pres-

sure, which can be estimated to be 7 MPa. Thus the total pressure estimated to prevail in the vault at the copper canister surface is then a maximum of 14 MPa.

The goal of this work was to study the general and pitting corrosion susceptibility of Cu OFP as well as the properties of surface films possibly forming on Cu OFP in the simulated saline groundwater conditions ($T = 80\text{ °C}$, $p = 14\text{ MPa}$). The goal was also to compare the results with the earlier study performed in highly saline groundwater.

2 EXPERIMENTAL

Oxygen free phosphorus containing copper (Cu OFP, 99.992 wt-% Cu and 45 ppm P, Outokumpu Poricopper Oy) was used as the test material in all the experiments. The working electrodes were polished using 4000 grit emery paper and rinsed with MILLI-Q® water before use. The experiments were performed in a static AISI 316 stainless steel autoclave having a volume of 5000 ml. The test specimens were introduced to the electrolyte which was then deaerated and pressurised to the test pressure using nitrogen gas (99.999%). During the experiments, nitrogen gas was continuously bubbled through the electrolyte in the autoclave. Based on experience, this procedure ensures the oxygen content to be lower than 5 mg/l. An external pressure balanced AgCl/Ag reference electrode filled with 0.1 M KCl was installed into the autoclave to enable potential measurement. Additionally, a Pd electrode saturated with hydrogen was used as a quasi-reference electrode and was assumed to behave as a Reversible Hydrogen Electrode (RHE). All the potentials in this work are reported on the standard hydrogen electrode

scale (SHE). The groundwater composition is given in Table I. This composition is representative of the saline groundwater. The solutions were made of p.a. chemicals and MILLI-Q® purified water. The pH of the solution was measured to be 8.40 after preparation and 8.30 to 8.36 in the autoclave after the tests. The pH estimated to prevail at the test temperature was 7.4 ± 0.7 (calculated from the potential difference of the AgCl/Ag- and RHE-electrodes).

Electrochemical impedance measurements were performed by a Solartron ECI 1287/FRA 1260 system controlled by ZPlot / CorrWare software (Scribner) in a frequency range 0.03 Hz...10 kHz at an AC amplitude of 10 mV (rms). Voltammetric and polarisation resistance measurements were performed with the same system. The contact electric resistance (CER) equipment was supplied by Cormet Ltd. Potentiostatic and potentiodynamic conditions during CER measurements were ensured using a Wenking LB 81M potentiostat and a Hi-Tek Instruments PPR1 waveform generator.

Table I. Composition of the groundwater (mg/l).

Cl ⁻	SO ₄ ²⁻	Mg ²⁺	Ca ²⁺	Na ²⁺	K ⁺	Br ⁻	F ⁻	Sr ²⁺	B ³⁺	I ⁻
14500	4.2	54.6	4000	4800	21	104.7	1.2	35.0	0.9	0.9

3 RESULTS AND DISCUSSION

3.1 Corrosion coupon tests

Three weight loss coupons were exposed to the environment. The coupons were weighed before and after the exposure. The exposure time was five days. After the exposure the specimen surfaces were examined with scanning electron microscopy (SEM) for possible pitting corrosion.

The surface appearance of the corrosion coupons is shown in Figs 1a to 1c. The appearance is typical for general corrosion. There was no sign of localised corrosion (pitting).

The weight loss measurement results are shown in Table II.

The general corrosion rate was calculated using the formula

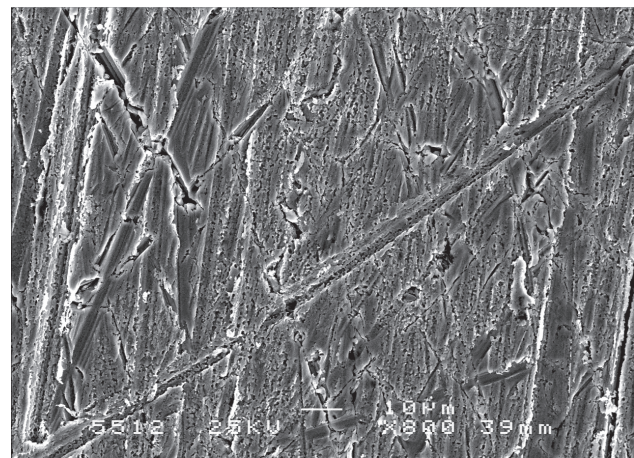
$$\Delta = \frac{\Delta m \cdot 3650}{\rho \cdot A \cdot t} [mm/y] \quad (1)$$

where Δm = weight loss [g], ρ = density [g/cm^3], A = surface area [cm^2] and t = exposure time [days]. The density of copper is $8.94 g/cm^3$.

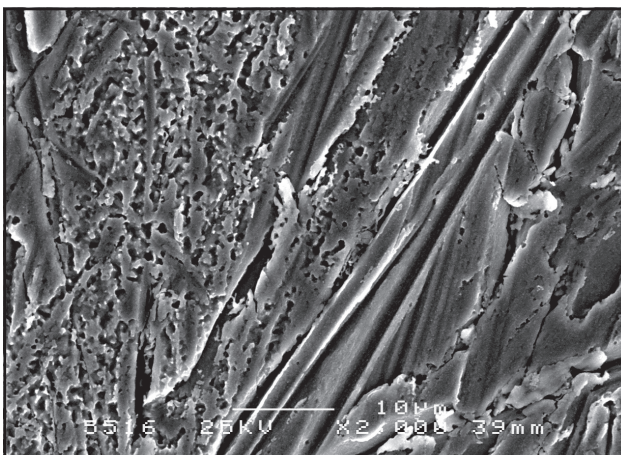
The calculated corrosion rates are in the average 0.014 ± 0.002 mm/y. Using a corrosion allowance of 30 mm this would indicate a lifetime of about 2100 years, assuming that the transport of

Table II. Corrosion coupon test results.

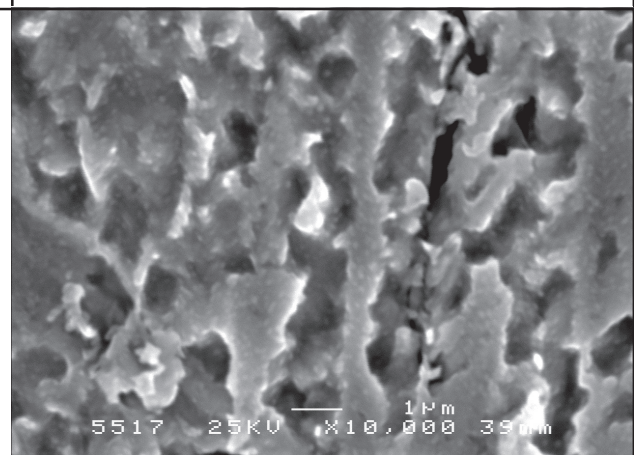
Specimen number	1	2	3
Surface area, cm^2	15.06	14.32	14.24
Weight before exposure, g	8.6878	6.7592	7.5096
Weight after exposure, g	8.6850	6.7565	7.5076
Weight loss, g	0.0028	0.0027	0.0020
Corrosion rate, mm/y	0.015	0.015	0.012



(a) Picture showing general dissolution features such as rounded edges of and breaks in the original polishing scratches, as well as small pore-like details. Magnification $\times 800$.



(b) Picture showing both a clearly dissolved area (left) and an only slightly dissolved area (right). Magnification $\times 2000$.



(c) Detail of the clearly dissolved area in picture (b) showing the small pore-like details. Magnification $\times 10000$.

Figure 1. Scanning electron microscopy images of the surface of Specimen No 1 after the five day exposure to the saline groundwater ($80^\circ C$, $14 MPa$).

corrosion products away from the surface and that of the reactants towards the surface would be similar to the present experimental situation. However, it is very likely that the rate of transport in bentonite clay is limited, and will possibly become rate limiting and thus slow down the corrosion process. The corrosion rate measured earlier [1] in highly saline groundwater (1.5 M or 53800 mg/l Cl⁻) but in otherwise similar conditions was 0.02 mm/y.

3.2 Voltammetry and polarisation resistance

The polarisation curve of Cu OFP in the test solution is shown in Fig. 2. The H⁺/H₂-equilibrium potential is at -0.47 V. In the figure, the range of corrosion potentials measured is also indicated, as well as the CuCl₂/Cu equilibrium potential (as calculated by Beverskog and Puigdomenech [2] for a concentration $[\text{Cu}(\text{aq})]_{\text{tot}} = 10^{-4}$ mol/kg, 1.5 molal Cl⁻). The corrosion potential is 0.1...0.2 V higher than the CuCl₂/Cu equilibrium potential. This reflects the fact that the corrosion potential is a mixed potential determined both by the anodic and cathodic reactions, i.e. oxidation of Cu to CuCl₂⁻ and reduction of O₂ (and/or H₂O). The cor-

rosion potential was about 0.1 V higher than that measured in the highly saline groundwater [1].

An increase of current is seen in Fig. 2 resulting in an anodic peak at about -0.02 V. A reduction peak is seen during the negative-going sweep at about $-0.35 \text{ V} < E < -0.2 \text{ V}$. The anodic peak at -0.02 V is due to an oxidation process, which could be dissolution of copper or formation of a copper containing surface film. Similar peaks were found in measurements performed in the highly saline groundwater [1]. However, the peaks found in the highly saline groundwater were roughly ten times lower in magnitude, although the same sweep rate (2 mV/s) was used. The peaks in the highly saline groundwater appeared at potentials about 0.1 V lower than in the present case, which is in accordance with the fact that also the corrosion potential was similarly lower by 0.1 V. The reason for the markedly lower anodic and cathodic peaks in the highly saline groundwater can not be concluded based on this work.

Figure 3 shows the polarisation curve of Cu OFP measured in a wider potential range extending to more positive potentials, $-0.47 \text{ V} < E < 0.53 \text{ V}$. A higher sweep rate was used to preserve the specimen as the current density at high positive potentials was found to be very high. The

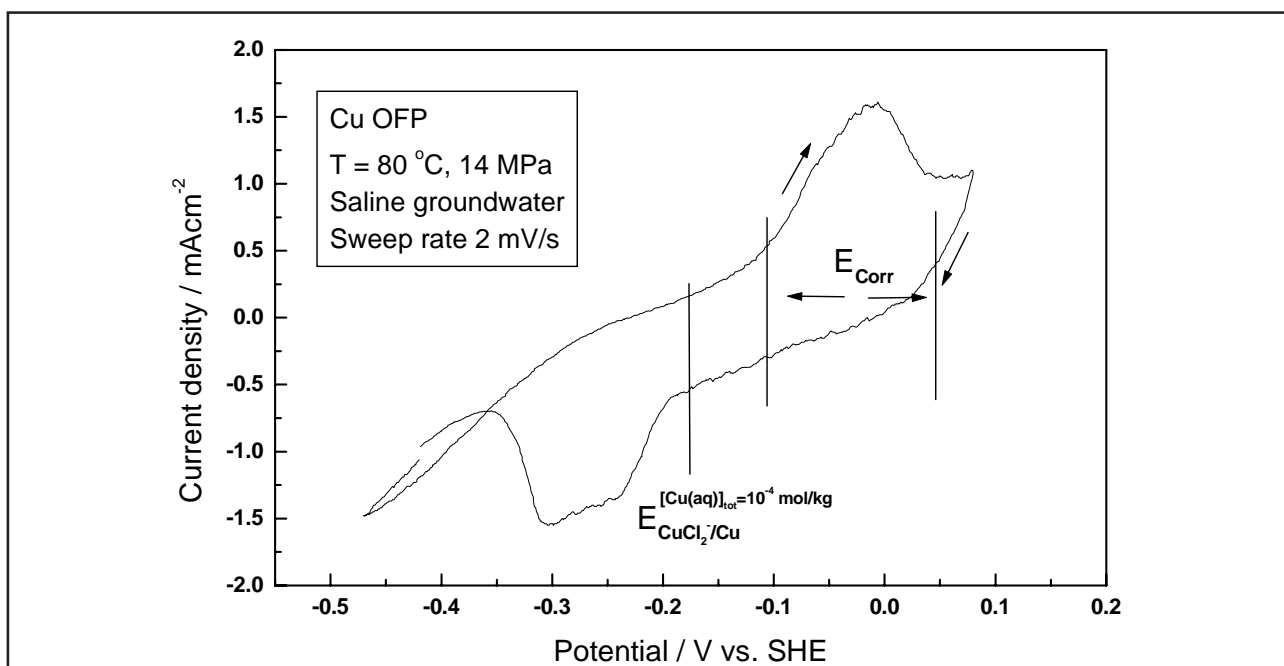


Figure 2. Polarisation curve of Cu OFP in simulated saline ground water at 14 MPa. $T = 80 \text{ }^\circ\text{C}$, sweep rate 2 mV/s (N_2 gas, continuous bubbling through the autoclave). Potential range $-0.47 \text{ V} < E < 0.07 \text{ V}$. Not corrected for i -R-drop.

small peak seen at -0.02 V with the lower sweep rate of 2 mV/s (Fig. 2) is not clearly seen with the higher sweep rate, partly because of the much larger scale, Fig. 3. The positive current increase starting at about 0.1 V reaches a level which is higher than 60 mAcm⁻² at $E = 0.4$ V, after which the current decreases rapidly as potential increases to 0.45 V. At still higher potentials the current increases again. In the negative going sweep a broad reduction peak is seen at 0.15 V $< E < 0.3$ V. According to the calculations of Beverskog and Puigdomenech [2], a solid compound of CuO (or at slightly lower pH also $\text{CuCl}_2 \cdot 3\text{Cu}(\text{OH})_2$) may be formed on copper in this environment at about $+0.3$ V. One may thus assume that the decrease in the current seen at about $+0.45$ V at the $\text{pH}_{T=80\text{C}} \approx 7.6$ is connected with a formation of a surface film of a composition close to CuO. It seems, though, that the film is not a real passive film in the sense that a high current still passes through it. The broad reduction peak at 0.15 V $< E < 0.3$ V is assumed to be connected with reduction of the non-passivating film formed at $E > 0.4$ V.

In the highly saline groundwater gain a similar behaviour was found [1]. However, the maximum current density was lower by about 50% and it was located at about 0.25 V, i.e. roughly 0.15 V

lower than in the present case. These results confirm that the behaviour of Cu OFP is rather similar in these two environments and that higher current densities are maybe unexpectedly found in the present case with lower salinity.

In open circuit potential decay experiments shown in Fig. 4 a plateau was found at $+0.35$ V. This indicates that at potentials higher than this a film is formed which is reduced at open circuit conditions at $+0.35$ V. The open circuit potential can only decrease further after this surface film has been at least partially reduced. A similar plateau was found also in the highly saline groundwater, but at a clearly lower potential of $+0.05$ V.

Polarisation resistance measurement is typically used to calculate corrosion rates. The procedure involves measurement of a potential-current curve so that the potential is deflected from the corrosion potential by typically $15\text{--}20$ mV in both positive and negative direction. Fig. 5 shows the measurement result after exposure time of 2 hrs and Fig. 6 the same after exposure time of 96 hrs. The polarisation resistance, R_p , as calculated from the data shown in Fig. 5 and Fig. 6 is about 1140 Ωcm^2 , and does not seem to depend on the exposure time.

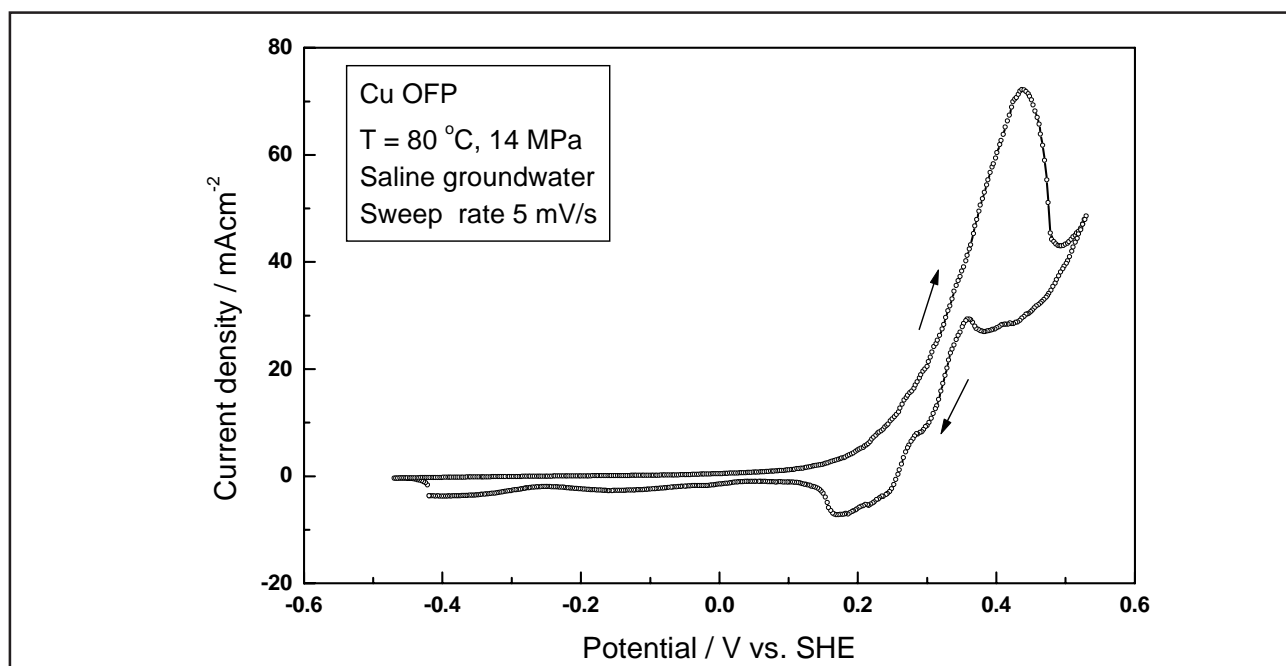


Figure 3. Polarisation curve of Cu OFP in simulated saline groundwater (N_2 gas, continuous bubbling through the autoclave) $T = 80$ °C, 14 MPa, sweep rate 5 mV/s, potential range -0.47 V $< E < 0.53$ V. Not corrected for i -R-drop.

3.3 Electric resistance of surface

The electric resistance was monitored together with the open circuit potential for a period of about 3 hrs. The very low electric resistance shown in Fig. 7 indicates that the surface has no passive film on it. Such a low electric resistance indicates a metallic surface with possibly some adsorbed anions. The open circuit potential in this exposure

was $E_{\text{corr}} \approx 0.04$ V. In highly saline groundwater [1] the behaviour at open circuit conditions was very similar to that found in the present work.

To study the effect of more oxidising environments the specimen was polarised to higher potentials with a sweep rate of 5 mV/s, Fig. 8. The resistance stayed at the very low level up to the potential $E \approx 0.4$ V. At higher potentials the resistance increased by 5 to 6 decades, indicating the

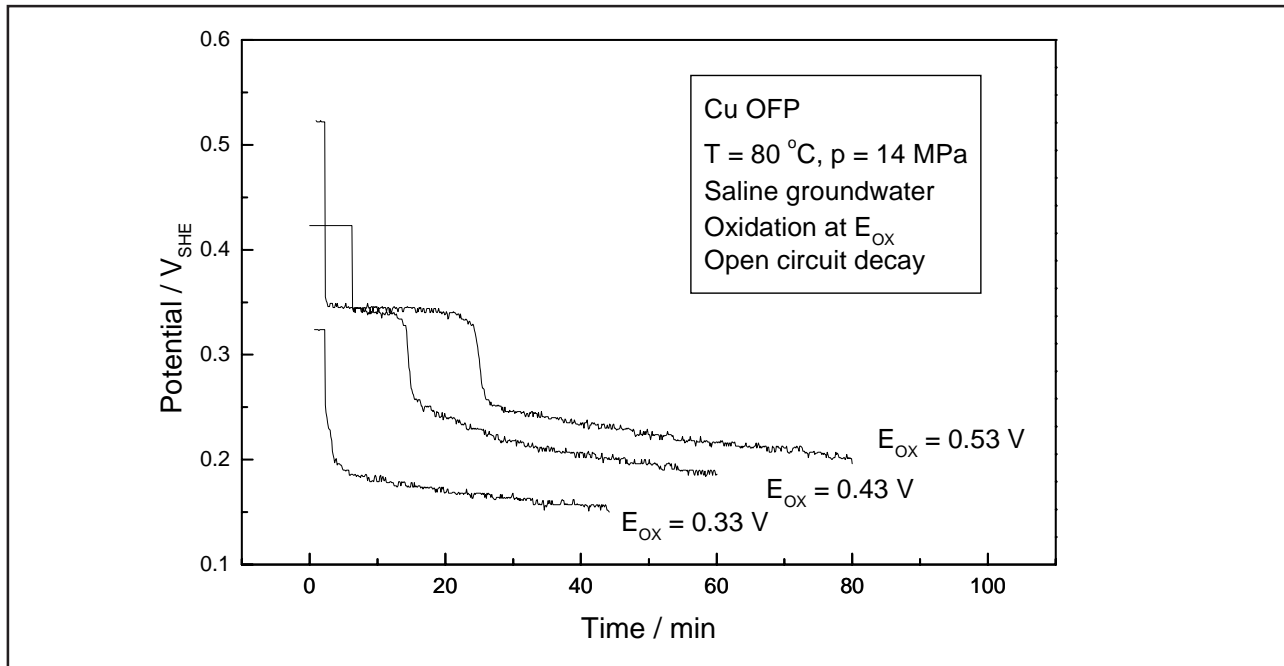


Figure 4. Open circuit potential decay after keeping the specimen at different elevated positive potentials.

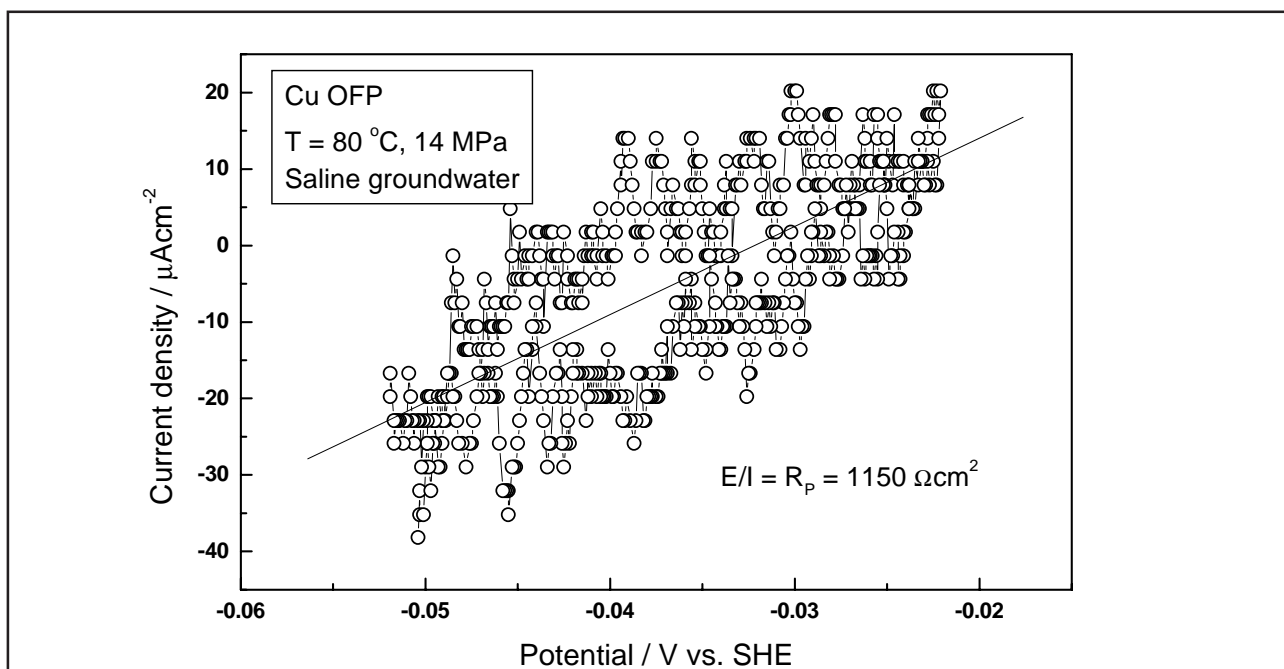


Figure 5. Polarisation resistance of Cu OFP in simulated ground water at 80 °C, 14 MPa, after exposure time of 2 hrs.

formation of a surface film. In the negative going sweep the resistance decreases at $E \approx 0.4$ V roughly from $5 \Omega\text{cm}^2$ to the level of $10^{-3} \Omega\text{cm}^2$. From this level the resistance decreased further down to the level of the almost clean surface when potential decreased below $E \approx 0.15$ V. In the highly saline groundwater [1] some indications of a surface film formation at very high potentials were detected, but not as clearly as in the present case.

3.4 Impedance response of copper

The impedance spectrum of Cu OFP in the test solution was measured at the corrosion potential, Fig. 9 and Fig. 10. The results indicate an impedance magnitude of about $1000 \Omega\text{cm}^2$ at the limit when $f \rightarrow 0$ Hz. In Fig. 9 the phase angle shows three processes. There is one maximum in the phase angle at about 500 Hz and another one at

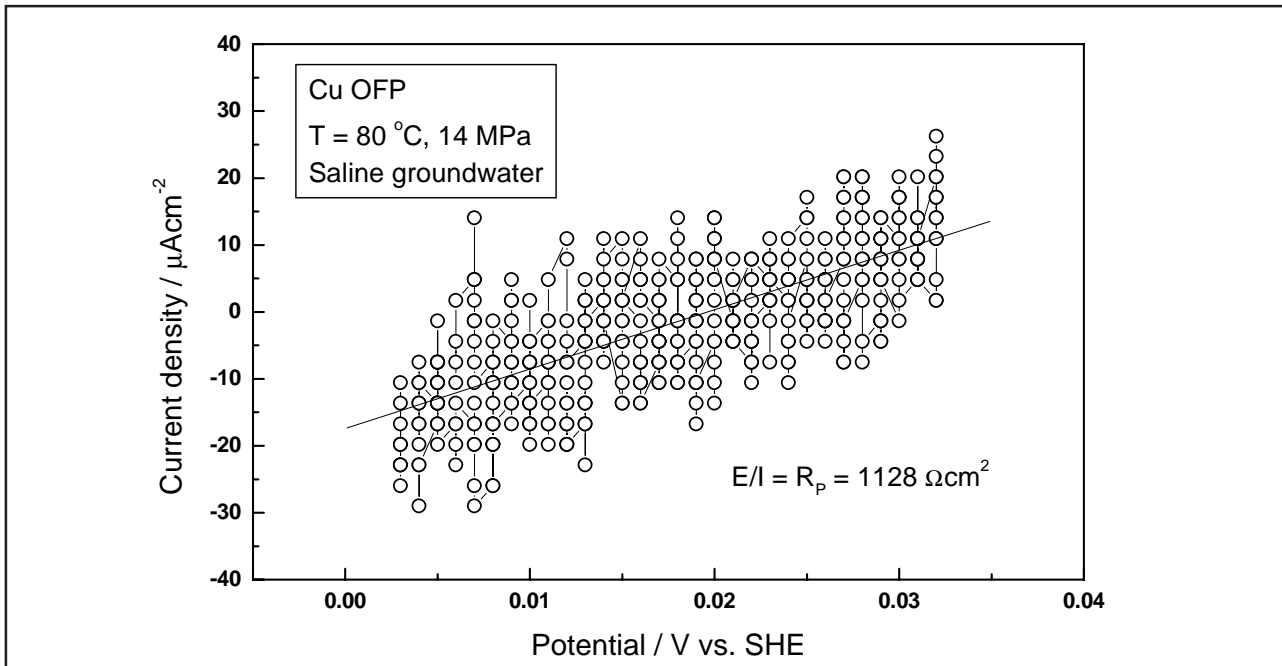


Figure 6. Polarisation resistance of Cu OFP in simulated ground water at 80 °C, 14 MPa, after exposure time of 96 hrs.

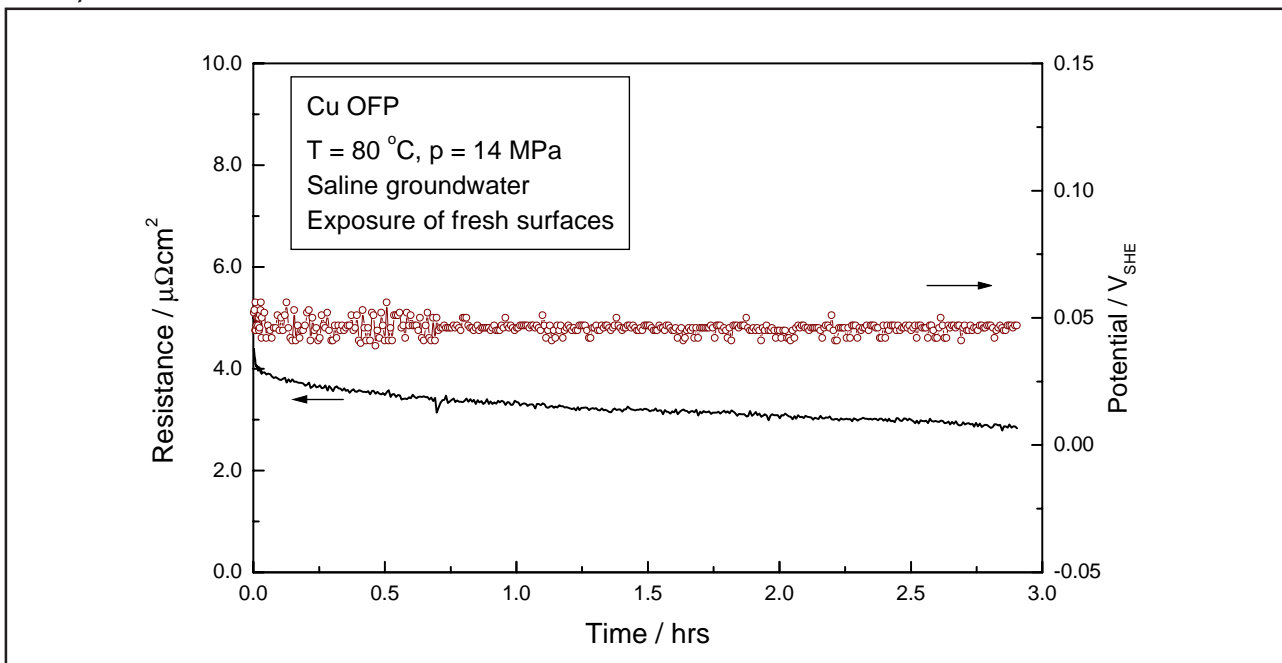


Figure 7. Electric resistance of Cu OFP fresh surfaces exposed to the simulated saline ground water at open circuit potential (E_{corr}).

about 20 Hz. At the lowest frequencies, i.e. at $0.02 \text{ Hz} < f < 0.2 \text{ Hz}$ there is an almost horizontal tail in the phase angle curve (also seen as a 45° straight line in the complex-plane plot, i.e. Nyquist-plot, see Fig. 10). This indicates a transport process (diffusion or migration). The results indicate a rather low magnitude of impedance of about $1000 \text{ } \Omega\text{cm}^2$ at the limit when $f \rightarrow 0 \text{ Hz}$. A passive film with good corrosion resistance, like that forming on Cr and Fe-Cr alloys in aqueous solutions has typically a magnitude of impedance in

the range $10^4 \text{ } \Omega\text{cm}^2 < |Z| < 10^6 \text{ } \Omega\text{cm}^2$ [3,4].

It was shown earlier [1] that there is no stable surface film on Cu OFP at the corrosion potential in highly saline groundwater. The voltammetric and CER results shown above indicate that in the present environment the situation is similar. Thus it is reasonable to assume that copper dissolution takes place at open circuit potential. Dissolution of copper may occur via different routes. As discussed earlier [1] there are two mechanisms of dissolution that explain equally well the experi-

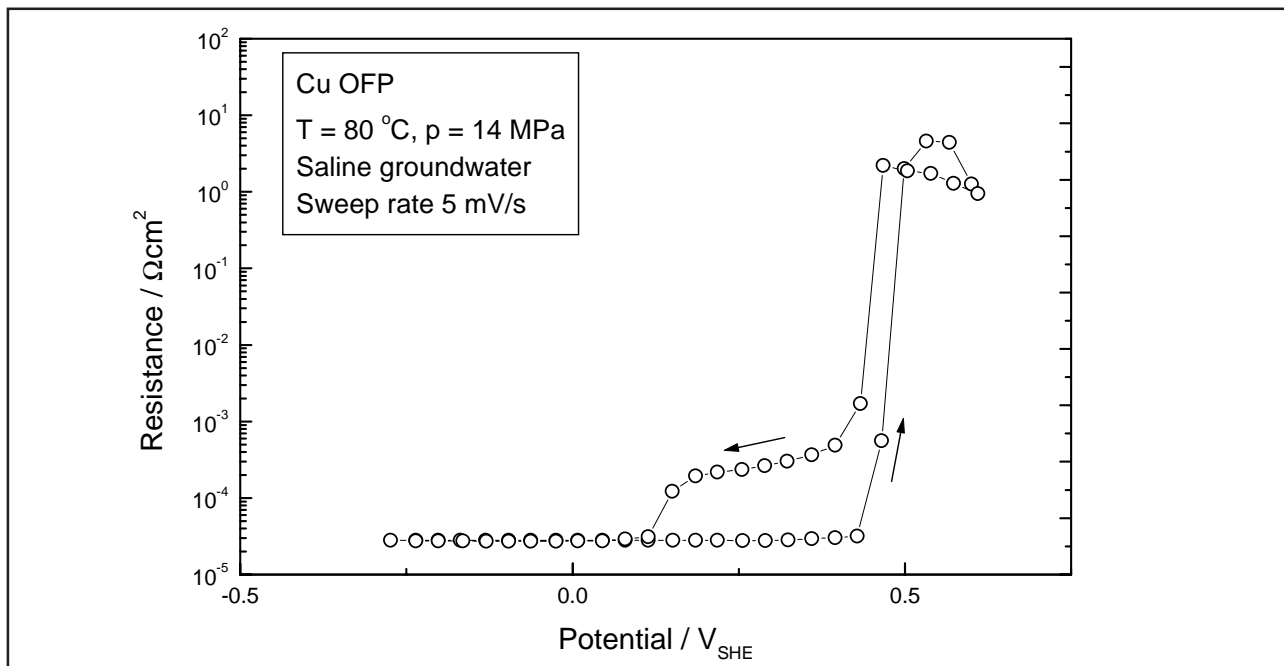


Figure 8. Electric resistance of Cu OFP as a function of potential in simulated saline ground water at $80 \text{ }^\circ\text{C}$, 14 MPa . Sweep rate 5 mV/s .

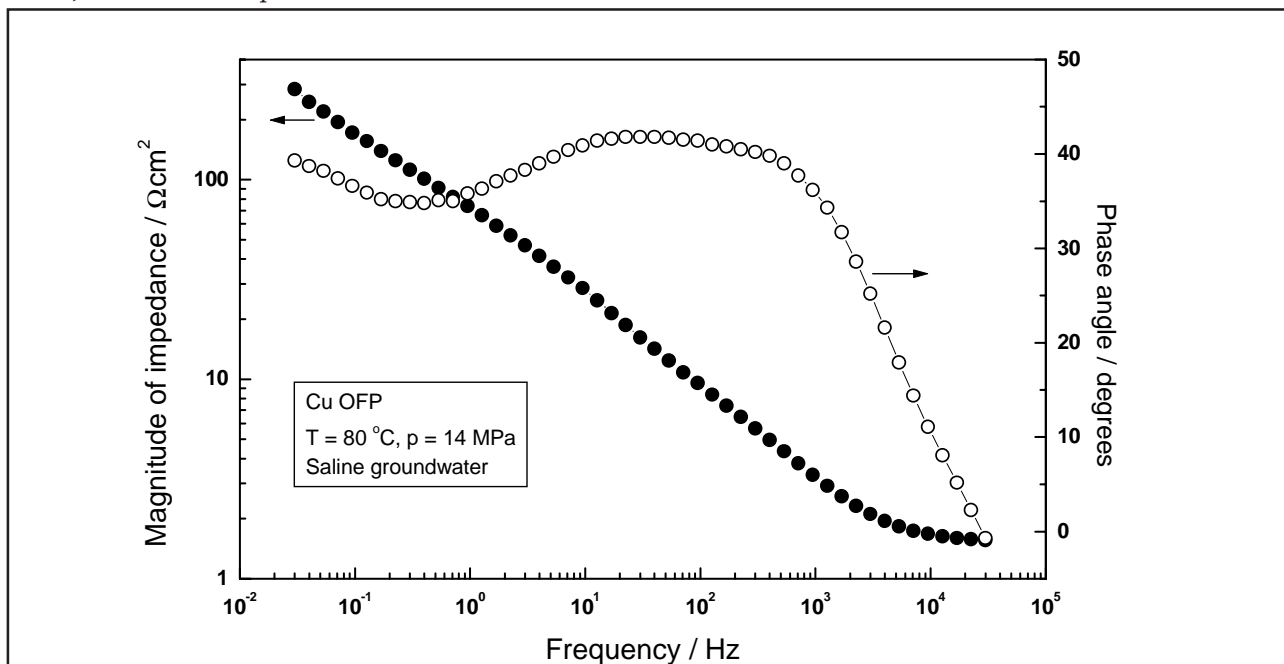
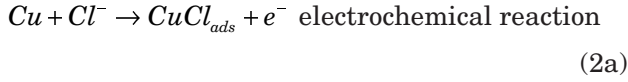


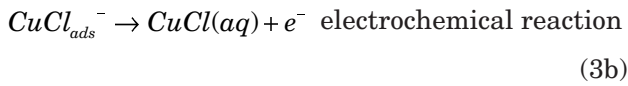
Figure 9. Impedance spectrum of Cu OFP in simulated ground water at $80 \text{ }^\circ\text{C}$, 14 MPa . Bode-plot.

mental results. The first one [5] is that copper reacts with Cl^- to form CuCl_{ads} on the surface, after which it combines with chloride to CuCl_2^- and diffuses further away into the solution. The reactions are as follows:



In this process the first step is electrochemical and the second chemical. King and Kolar in their review [7] and King and Tang [8] indicate that their data ($\text{Cl}^- < 1 \text{ M}$) is best fitted by the above reaction scheme 2a/2b.

Gabrielli et al. [6] have proposed, based on recent experimental evidence, that the process of copper dissolution in neutral solutions proceeds as follows:



The same equivalent circuit can describe both the reaction schemes 2a/2b and 3a/3b. The difference is that in the reaction scheme 2a/2b the first reaction, being an electrochemical one, should depend on potential and the resistance associated with it should decrease as potential increases. On the other hand, the resistance of a chemical reaction

should not depend on potential. In the present work the effect of potential was not investigated. However, in earlier work in highly saline groundwater it was shown [1] that the impedance magnitude decreased as potential increased, indicating that second step in the process is an electrochemical one. Based on this the process sequence proposed by Gabrielli et al. [6] is considered to be the correct one in the present case as well.

The equivalent circuit is shown in Fig. 11. Here R1 is the resistance of the electrolyte, R2 is the resistance of the chemical reaction, C1 the capacitance of the adsorption free surface, R3 the charge transfer resistance, CPE2 the imperfect capacitance of the part of surface with adsorbed $\text{CuCl}_{\text{ads}}^-$ and R_w the resistance of the transport process (described by the Warburg impedance W_s). In this scheme the Warburg impedance describes the transport of the reaction product $\text{CuCl}(\text{aq})$ away from the surface. The magnitudes of the parameters calculated with this equivalent circuit are shown in Table III.

The following equation relates the capacitance C with the distance d of the capacitor surfaces (here ϵ and ϵ_0 are the permittivity coefficient of the medium and permittivity of vacuum, respectively)

$$C = \frac{\epsilon \cdot \epsilon_0 \cdot A}{d} \quad (4)$$

Based on this equation, the capacitance value (C_2

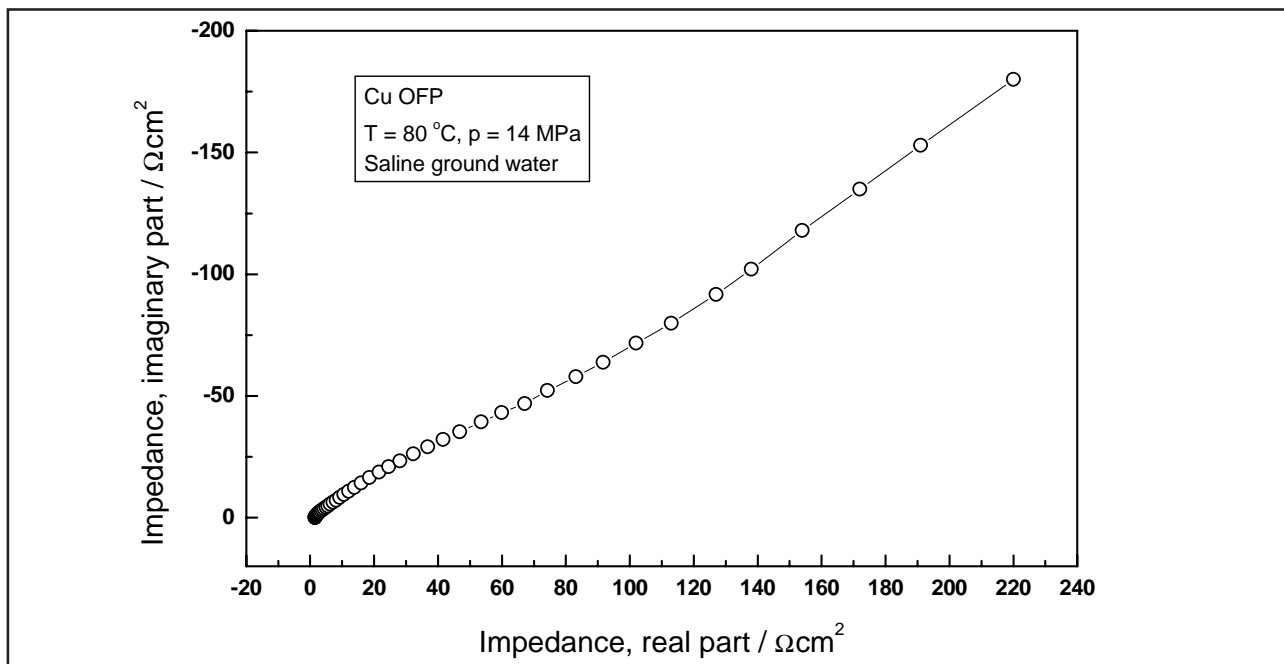


Figure 10. Impedance spectra of Cu OFP in simulated ground water at 80 °C, 14 MPa. Complex-plane (Nyquist) plot.

Table III. Best-fit parameters for the impedance spectra of Cu OFP measured at open circuit Cu OFP in highly saline groundwater at $T = 80\text{ }^{\circ}\text{C}$.

E_{CORR}	R_1 $\Omega\text{ cm}^2$	R_2 $\Omega\text{ cm}^2$	R_3 $\Omega\text{ cm}^2$	C_2 $\mu\text{F cm}^{-2}$	R_w $\Omega\text{ cm}^2$
+0.05 V	1.6	2.3	140	50	2160

= $50\text{ }\mu\text{Fcm}^{-2}$) in Table III and using $\epsilon = 100$ the distance d can be approximated to be $3.5\text{ }\text{\AA}$, which indicates that this capacitance is related to the Helmholtz layer. The capacitance related to the CPE2 could not be estimated due to the heavy distortion of the element, i.e. it did not behave as a real capacitor. This is probably because the adsorption sites are unevenly distributed over the surface.

From corrosion point of view, the process which shows the highest resistance becomes rate limiting. In this case, using the model of Fig. 11 for interpretation of the impedance data the rate limiting process is the transport process, having a resistance of the order of $2160\text{ }\Omega\text{cm}^2$. This value is reasonably close to the value given by the polarisation resistance measurement (Figs 5 and 6), $R_p = 1140\text{ }\Omega\text{cm}^2$. This indicates that the polarisation resistance, in which measurement frequency corresponds roughly to $5 \cdot 10^{-3}\text{ Hz}$, is likely to be dominated by the same transport process. However, it is also possible that the rate of the process is limited by the cathodic reaction. Because of the

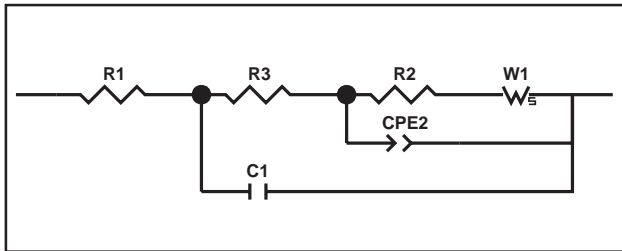


Figure 11. Equivalent circuit for the corrosion reaction scheme.

very low oxygen content in the solution the diffusion of oxygen to the surface may in this case be the rate-limiting step.

Ogundele and Jain [9] determined the corrosion rate of CuOFP in the Standard Canadian Shield Saline Solution (SCSSS, $0.97\text{ M Cl}^- \cong 34400$ ppm, atmospheric pressure, nitrogen bubbling) by an accelerated electrochemical technique, specifically determination of Tafel slopes (voltage-current curves) within $\pm 15\text{ mV}$ from the open circuit potential. From the polarisation resistance measurement they estimated that the corrosion rate at $75\text{ }^{\circ}\text{C}$ at $\text{pH}_{\text{RT}} = 7$ is 0.0024 mm/y . In their tests the corrosion rate at $75\text{ }^{\circ}\text{C}$ was almost constant when pH was varied from 4 to 10. Reanalysing the data from Ogundele and Jain [9] one arrives at a value for the polarisation resistance of $R_p \approx 30000\text{ }\Omega\text{cm}^2$. This is about 30 times higher than that measured in the present work. This may be due to the difference in the groundwater chemistry, the pressure of the environment (0.1 MPa vs. 14 MPa), the difference in the temperature ($75\text{ }^{\circ}\text{C}$ vs. $80\text{ }^{\circ}\text{C}$) or salinity (0.97 M vs. 0.4 M Cl^-). Increase in pressure or temperature is expected to increase the measured corrosion rate. The corrosion rate calculated by Ogundele and Jain [9] is roughly 6 times lower than that measured in this work. The approach of calculating corrosion rate from polarisation resistance using Tafel coefficients as done by Ogundele and Jain [9] is correct assuming that the anodic process is charge transfer controlled. However, in the present work we have shown that charge transfer resistance is much smaller than transport resistance (Table III). This means that the anodic process is most likely under transport resistance control and that corrosion rate estimated based on the polarisation resistance data is probably incorrect.

4 CONCLUSIONS

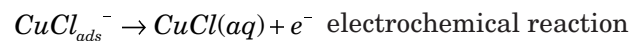
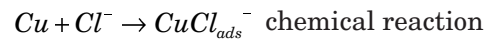
The conclusions presented here are strictly applicable only for the present case, where the groundwater was deoxygenated with nitrogen bubbling (ensuring dissolved oxygen level of lower than 5 mg/l) and where there was almost no mass transfer limitation for the corrosion products away from the surface. The main conclusions made are:

The corrosion potential of Cu OFP in all test runs was in the range of $-0.10 V_{\text{SHE}} < E_{\text{corr}} < 0.05 V_{\text{SHE}}$, i.e. about 0.1 V higher than in the highly saline groundwater.

At the corrosion potential active dissolution (corrosion) of Cu OFP takes place, as was the case in highly saline groundwater. However, the corro-

sion rate based on weight loss measurements of corrosion coupons was 0.014 mm/y, about 30% lower than in the highly saline groundwater.

The mechanism of copper dissolution in saline groundwater at 80 °C and 14 MPa is suggested to occur via the same reactions as in the highly saline groundwater [1], i.e.



where the reaction intermediate $\text{CuCl}_{\text{ads}}^-$ is adsorbed onto the surface and is then further oxidised to $\text{CuCl}(\text{aq})$.

REFERENCES

- 1 Laitinen T, Mäkelä K, Saario T, Bojinov M. Susceptibility of copper to general and pitting corrosion in highly saline groundwater, SKI Report 01:2. Swedish Nuclear Power Inspectorate, Stockholm, 2001. 24 p.
- 2 Beverskog B, Puigdomenech I. Pourbaix diagrams for the system copper-chlorine at 5–100 °C. SKI Report 98:19, 1998. Swedish Nuclear Power Inspectorate, Stockholm. 18 p. + app. 16 p.
- 3 Bojinov M, Fabricius G, Laitinen T, Saario T, Sundholm G. Conduction mechanism of the anodic film on chromium in acidic sulphate solutions. *Electrochimica Acta*. Vol. 44 (1998) No: 2–3, 247–261
- 4 Bojinov M, Fabricius G, Laitinen T, Mäkelä K, Saario T, Sundholm G. Conduction mechanism of the anodic film on Fe–Cr alloys in sulphate solutions. *Journal of the Electrochemical Society*. Vol. 146 (1999) No: 9, 3238–3247.
- 5 Deslouis C, Tribollet B, Mengoli G, Musiani M. Electrochemical behaviour of copper in neutral aerated chloride solution. I. Steady-state investigation. *Journal of applied electrochemistry*, Vol 18, pp. 374–383, 1988.
- 6 Gabrielli C, Keddam M, Minouflet-Laurent F, Perrot H. Simultaneous EQCM and ring-disc measurements in AC regime. Application to copper dissolution. *Electrochemical and solid-state letters*, Vol. 3, pp. 418–421, 2000.
- 7 King F, Kolar M. Prediction of the lifetimes of copper nuclear waste containers under restrictive mass-transport and evolving redox conditions. *Corrosion NACE 1995*, paper No. 425, 28 p.
- 8 King F, Tang Y. The anodic dissolution of copper in chloride–sulphate groundwaters. Report No 06819-REP-01200-0058 R00. Ontario Hydro, Nuclear Waste Management Division. Toronto. 35 p. + app. 15 p. August 1998.
- 9 Ogundele G, Jain D. Abiotic corrosion of Finnish OFP copper in standard Canadian Shield saline solution (SCSSS). Report No 06819-REP-01200-0057R00. Ontario Hydro, Nuclear Waste Management Division. Toronto. 32 p. + app. 17 p. June 1998.